Cell Reports
Physical Science

CellPress
OPEN ACCESS

Article

Seeded growth of adaptive tiles on DNA origami

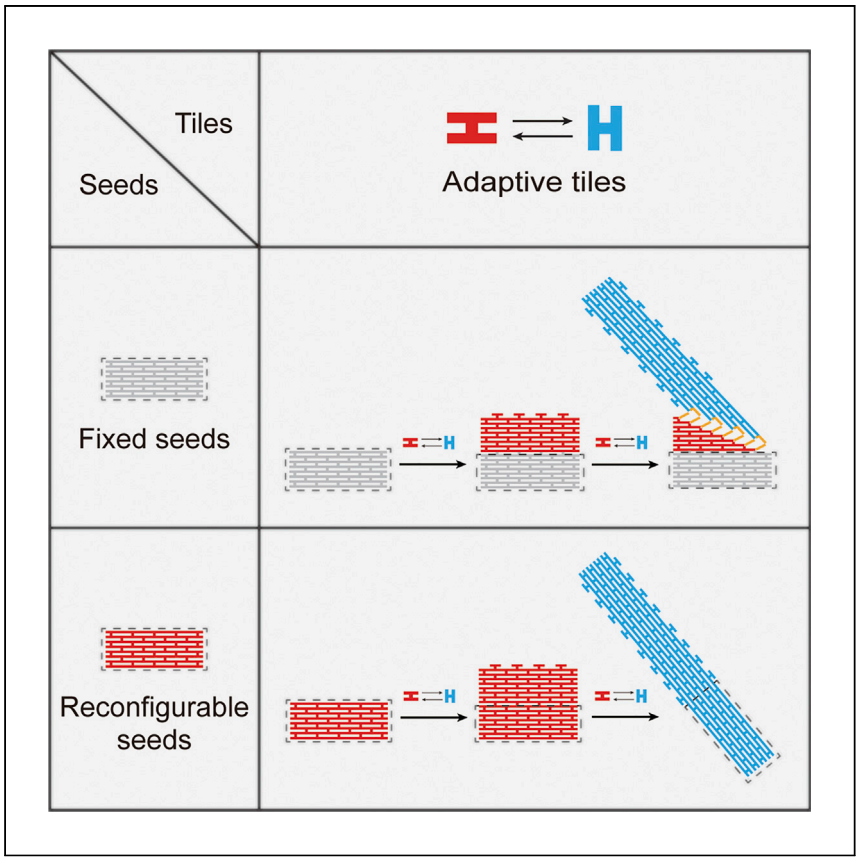

Liu et al. develop a seeded growth strategy whereby adaptive DNA tiles can adaptively assemble on DNA origami seeds, with their shapes changing simultaneously. When the adaptive tiles assemble on reconfigurable seeds, the seeds change into the other conformation, with the transformation triggered by the growing tile lattice.

Yan Liu, Jin Cheng, Yuqi Wang, ..., Daxiang Cui, Yonggang Ke, Jie Song

yonggang.ke@emory.edu (Y.K.)
sjie@sjtu.edu.cn (J.S.)

Highlights

The shapes of adaptive tiles can change to match "red" or "blue" DNA origami seed

The adaptive tiles can transform to "blue" conformation when assembling on fixed seed

The adaptive tile can trigger the deformation of reconfigurable seed

A molecular "tug-of-war" occurs when adaptive tile assembling on reconfigurable seed

Liu et al., Cell Reports Physical Science 3, 101040
September 21, 2022 © 2022 The Author(s).
https://doi.org/10.1016/j.xcrp.2022.101040

Please cite this article in press as: Liu et al., Seeded growth of adaptive tiles on DNA origami, Cell Reports Physical Science (2022), https://doi.org/10.1016/j.xcrp.2022.101040

Cell Reports
Physical Science

CellPress
OPEN ACCESS

Article

Seeded growth of adaptive tiles on DNA origami

Yan Liu,[1] Jin Cheng,[1,2] Yuqi Wang,[1] Bin Ji,[1,2] Linlin Tang,[1] Kexuan Zou,[1] Yujie Xie,[3] Daxiang Cui,[1] Yonggang Ke,[4,*] and Jie Song[1,5,6,*]

SUMMARY

Structural DNA nanotechnology has been applied to construct complex static and dynamic DNA structures. Seeded growth, intended to regulate the crucial nucleation step, has been used to control the assembly of DNA tiles. However, most of the seeded growth strategies were applied to fixed DNA tiles, whereas the seeded growth on dynamic DNA tiles remains unreported. Here, we propose a seeded growth strategy in which dynamic tiles adaptively change their shapes to match the architecture of a DNA origami seed. Furthermore, when more adaptive DNA tiles assemble on a reconfigurable DNA origami domino array (DODA) seed, the conformation of DODA seeds is reversibly affected by the spontaneous reconfiguration of adaptive tiles. The adaptive seeded growth provides a mechanism for the construction of complex DNA nanomachines and may offer a general and adaptable method for the advancement of responsive materials, with active, autonomous, and adaptive spatiotemporal control properties.

INTRODUCTION

Structural DNA nanotechnology has undergone great advancements during the past 4 decades, since the conceptual foundation by Nadrian Seeman in the 1980s.[1–3] Currently, powerful design strategies, such as DNA origami[4] and DNA bricks,[5–7] are applied to construct complex static and dynamic DNA structures,[8] ranging from one-dimensional (1D),[9] 2D,[10] to 3D.[11] Nonetheless, it has become increasingly challenging to produce DNA structures of even more massive physical size and molecular weight by using a one-pot self-assembly of fully addressable nanostructures, which faces issues of higher cost and lower yields.[12] Therefore, various strategies, including the hierarchical assembly of DNA supramolecular structures,[10,13,14] DNA crystal,[15–18] and DNA seeded growth,[19–21] have been developed for the fabrication of DNA structures of increasing molecular mass and physical size,[22] providing potent platforms for addressing even more tasks.[12]

Seeded growth is commonly found in the crystal growth of inorganic and organic compounds,[23,24] in which the seeds are served as stable nucleus and templates to quickly produce large and well-defined crystals.[25] In structural DNA nanotechnology, long DNA strands,[21,26] DNA tiles,[27,28] and DNA origamis[15,29–31] are extensively used as the seeds for controlling the assembly of DNA tiles. The presence of seeds can significantly reduce the nucleation free-energy barrier[20,26,28] and induce the tiles to predetermine the assembly route. Specifically, the architectural features such as rigidity, geometry, and complementarity could be individually tailored between DNA seeds and DNA tiles, allowing for easily implementing many tasks such as DNA computing,[25,32] nucleation mechanism[28] or pathway exploring,[19,29] and landmarks (seeds) connecting.[33]

[1]Institute of Nano Biomedicine and Engineering, Department of Instrument Science and Engineering, School of Electronic Information and Electrical Engineering, Shanghai Jiao Tong University, 800 Dongchuan Road, Shanghai 200240, P.R. China

[2]Wuxi Center for Disease Control and Prevention, Wuxi, Jiangsu 214023, P.R. China

[3]School of Medicine, Shanghai University, Shanghai 200444, P.R. China

[4]Wallace H. Coulter Department of Biomedical Engineering, Georgia Institute of Technology and Emory University, Atlanta, GA 30322, USA

[5]Institute of Basic Medicine and Cancer (IBMC), Chinese Academy of Sciences, The Cancer Hospital of the University of Chinese Academy of Sciences, Hangzhou, Zhejiang 310022, P.R. China

[6]Lead contact

*Correspondence: yonggang.ke@emory.edu (Y.K.), sjie@sjtu.edu.cn (J.S.)

https://doi.org/10.1016/j.xcrp.2022.101040

This is an open access article under the CC BY-NC-ND license (http://creativecommons.org/licenses/by-nc-nd/4.0/).

Please cite this article in press as: Liu et al., Seeded growth of adaptive tiles on DNA origami, Cell Reports Physical Science (2022), https://doi.org/10.1016/j.xcrp.2022.101040

In this work, we introduce a unique seeded growth of the adaptive DNA tiles on DNA origami seeds: The free tiles conformations are undetermined until they crystallize onto the seed structures. The adaptive DNA tiles are designed through the assembly of 4-arm junction units based on our previous work.[34,35] Because of the mobile nicking points at the boundary, the tiles are in an unstable state, possessing a red or blue configuration. After binding with the two conformational origami seeds (shown as red and blue), the nicking points are removed, and the tiles are capable of changing themselves to the corresponding conformations, thus assembling on the seeds. First, the assembly of adaptive DNA tiles on a fixed DNA origami seed is studied, showing that the adaptive tiles can assemble on both "red" origami seed and "blue" origami seed. Second, we compare seeded adaptive tile assembly and spontaneous nucleation and assembly without seeds. In low tiles concentration, the tiles assemble following the designed pathways. With more tile assembling on the fixed seed, the tiles lattice starts to transform into the other conformation. Finally, the investigation of adaptive growth is carried out by using reconfigurable DNA origami domino array (DODA) seeds, whose conformation can be reversibly affected by tile adaptive assembly. The DODA seeds are designed based on our previous studies,[34,35] which can be reconfigured between two stable configurations. Because the DODA seeds themselves can be transformed, an interesting molecular "tug-of-war" is observed during the growth of adaptive tiles on these seeds. The adaptive growth represents a new strategy for seeded DNA self-assembly, and can also provide a new mechanism for the construction and regulation of complex DNA nanomachines.

RESULTS

Assembly of adaptive DNA tiles on DNA origami seeds

To evaluate the reconfigurable ability, both the adaptive DNA tiles and the fixed DNA tiles were used to assemble on the origami seeds (Figures 1 and S1–S3). Similar to the traditional nucleation and growth strategy,[20,21,25] the fixed DNA tiles (marked as gray tiles in Figure 1A) could successfully grow on the origami seeds under optimized incubation temperature and further confirmed by atomic force microscopy (AFM) with lengths up to approximately 200 nm (Figures S4–S8). Those tile structures were specially designed to fix the pattern of reserved DNA origami seed, and apparently failed to grow on other different origami seeds (Figures S9 and S10). Compared with the above fixed tiles, we used dynamic "4-arm" junction DNA tiles (here, two conformations shown as red and blue tiles in Figure 1B) to explore their assembly on the origami seeds. The detail design information was shown in Figure S11. For those adaptive DNA tiles, the incubation temperature of the tile growth on origami seeds was optimized at approximately 60°C (Figures S12–S17). Next, the adaptive DNA tiles were used to assemble on two kinds of DNA origami seeds (also marked as red and blue in Figure 1B). Through AFM images, the adaptive DNA tiles could successfully grow on both of the two different origami seeds (Figures 1B and S18–S22). The length of those assembly structures is approximately 150 nm on red origami seeds and approximately 300 nm on blue origami seeds, as shown in the statistical diagram of Figure 1B, which should be due to the different aspect ratio of the red and blue adaptive DNA tiles. In addition, the tiles without the seeds may prefer to assemble into tube-like structures (Figures S23–S25). The aforementioned results showed that the adaptive DNA tiles possess the capability of reconfigurability and could adaptively change their shapes to match the architecture of the DNA origami seeds.

Regulable growth of adaptive DNA tiles on origami seeds via controlling nucleation rate

Next, we further investigated how spontaneous nucleation of tiles could affect the assembly process (Figure 2). Because the nucleation rates or nucleation kinetics

Please cite this article in press as: Liu et al., Seeded growth of adaptive tiles on DNA origami, Cell Reports Physical Science (2022), https://doi.org/10.1016/j.xcrp.2022.101040

CellPress
OPEN ACCESS

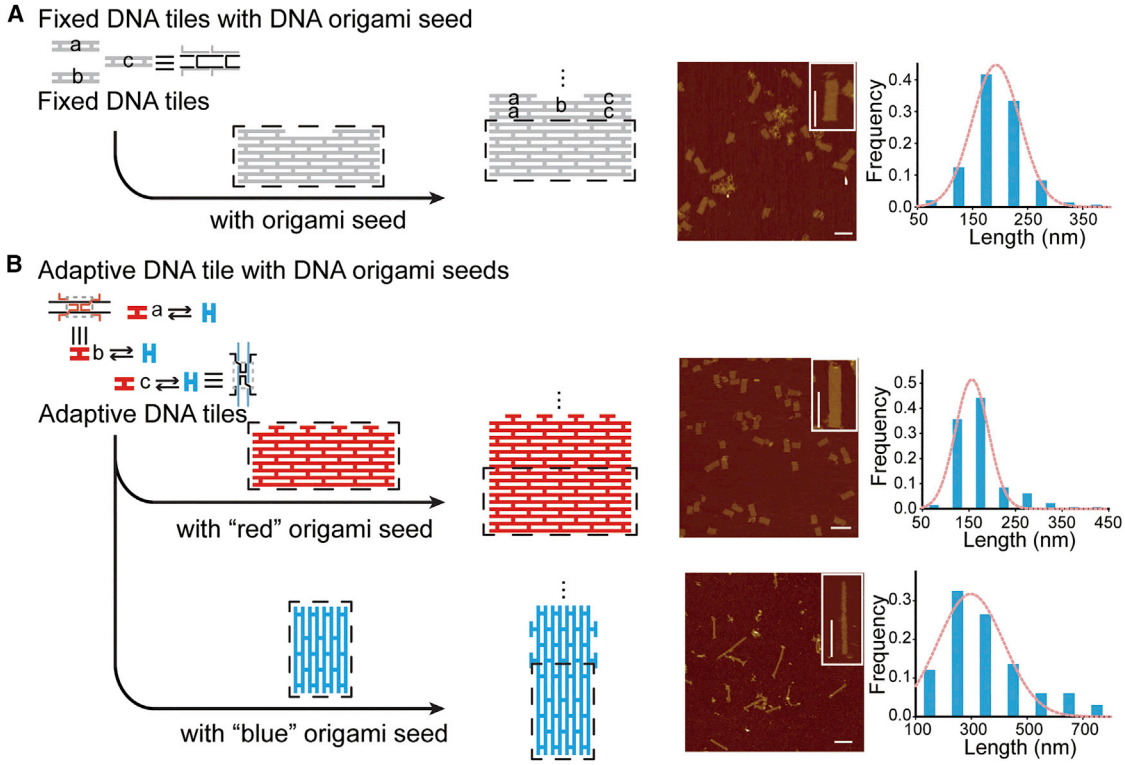

Figure 1. Assembly of adaptive DNA tiles on DNA origami seeds

(A) Fixed DNA tiles assembly on DNA origami seeds. Scale bars: 100 nm.

(B) Adaptive DNA tiles assembly on 2 DNA origami seeds. AFM images and yield analysis were completed using 100 nM fixed or adaptive DNA tiles assembly on DNA origami seeds. Scale bars: 100 nm.

can be influenced by the monomer concentrations,[28,36] we used a series of tiles concentrations to control the nucleation rates (Figure 2A). To better characterize the nucleation process, the fixed seeds with a larger size (twice as large as the one in Figure 1) were selected, while the adaptive DNA tiles were the same as the one used in Figure 1, prompting assembly on partial area of the fixed seeds (Figure S26). The assembled fixed seeds were imaged by AFM (Figure S27) and then used to react with different concentrations of adaptive DNA tiles. In low tiles concentrations (<100 nM), the nucleation rate was slow, and adaptive DNA tiles assembled following the red conformation pathway, which was dominated by the fixed seeds (Figures 2A–2I). From the AFM images in Figures 2B, 2C, and S28, the adaptive DNA tiles successfully grew on the fixed origami seeds, with their conformation mainly remaining in red. The average length of the assembled structures was approximately 125 nm, and the yield of the structures in red conformation was >90%, as demonstrated in the statistical analysis of Figure 2C.

As demonstrated in the previous paper,[37,38] different nucleation rates could affect the morphology and size of the crystals. Therefore, we further explored whether high nucleation rates of the adaptive tiles could regulate the growth process on fixed origami seeds. By increasing the concentration of the adaptive DNA tile to 200 nM, the nucleation rates slightly increased, and blue configuration structures occasionally resulted in low productivity, which indicated a possibility for the regulable growth on fixed seeds (Figures S29 and S30). Furthermore, with an adequate amount of adaptive DNA tiles (>300 nM), the spontaneous nucleation rate was high, and

Please cite this article in press as: Liu et al., Seeded growth of adaptive tiles on DNA origami, Cell Reports Physical Science (2022), https://doi.org/10.1016/j.xcrp.2022.101040

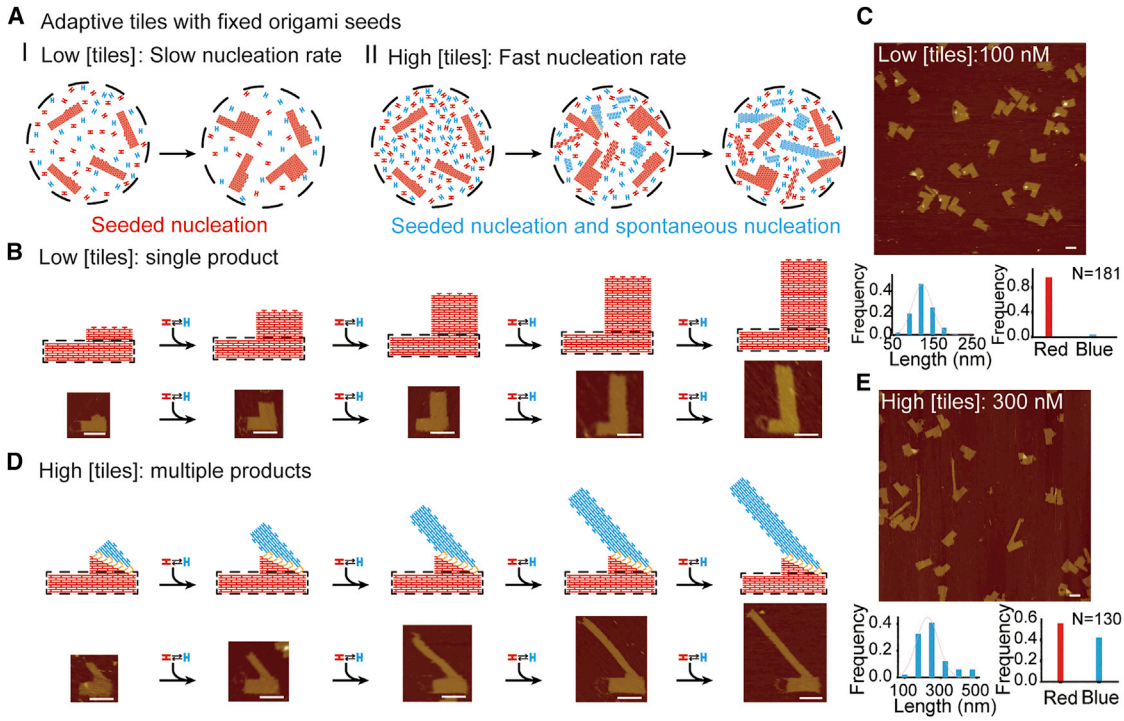

Figure 2. Regulable growth of adaptive DNA tiles on fixed origami seeds via controlling nucleation rate

(A) Adaptive DNA tiles assembly on fixed origami seeds.

(B and C) Low concentration of adaptive DNA tiles assembly on fixed seeds (B) and (C) their yield analysis. The growth was induced by seeds with the adaptive DNA tiles assembly following the red conformation pathway. Scale bars: 100 nm.

(D and E) High concentration of adaptive DNA tiles assembly on fixed seeds (D) and (E) their yield analysis. Adaptively structural transformation to blue configuration gradually occurred with the increase in adaptive DNA tiles. Note that on the left was the yield of blue structures and on the right was the yield between 2 structures. During the transformation of the assembled structures, some of the units are reconfigured to the blue conformation, while some units are still in the red conformation. Due to the geometry of the units, red conformation and blue conformation units are always bridged by partially open intermediate units, and the continuous transformations propagated through a diagonal pathway. Scale bars: 100 nm.

adaptive tiles nucleated and grew following both red and blue conformation pathways due to the coexistence of the seeded nucleation and spontaneous tiles nucleation (Figure 2A-II). Other than the structures in red, the representative AFM images of blue conformation structures also demonstrated the effective assembly of adaptive DNA tiles on fixed seeds and the realization of the regulable growth of adaptive DNA tiles on fixed seeds (Figures 2D and 2E). Meanwhile, the statistical analysis of the assembled structures was done according to the AFM images in Figures S31–S33, demonstrating that the structures grew up to 500 nm in the blue conformation, with an average length of approximately 300 nm (Figure 2E). Moreover, the yield between the red conformation and the blue conformation structures was also analyzed, and the yield of blue conformation structures was nearly 40% (Figure 2E).

Seeded growth of adaptive DNA tiles on reconfigurable DNA origami seeds with tug-of-war behavior

Compared to the fixed seeds, a reconfigurable DODA seed that could be reconfigured between two stable configurations was introduced to evaluate whether the seeded growth process could regulate the configurational changes in DODA seeds (Figure 3A, dashed box). To realize the robust assembly, the DODA seed was designed in equal proportion to the adaptive tiles. Similar to the growth on fixed seeds, the growth process was regulated by different concentrations of adaptive tiles assembling on the DODA seeds (Figure 3). In low tiles concentrations (200 nM),

Please cite this article in press as: Liu et al., Seeded growth of adaptive tiles on DNA origami, Cell Reports Physical Science (2022), https://doi.org/10.1016/j.xcrp.2022.101040

CellPress
OPEN ACCESS

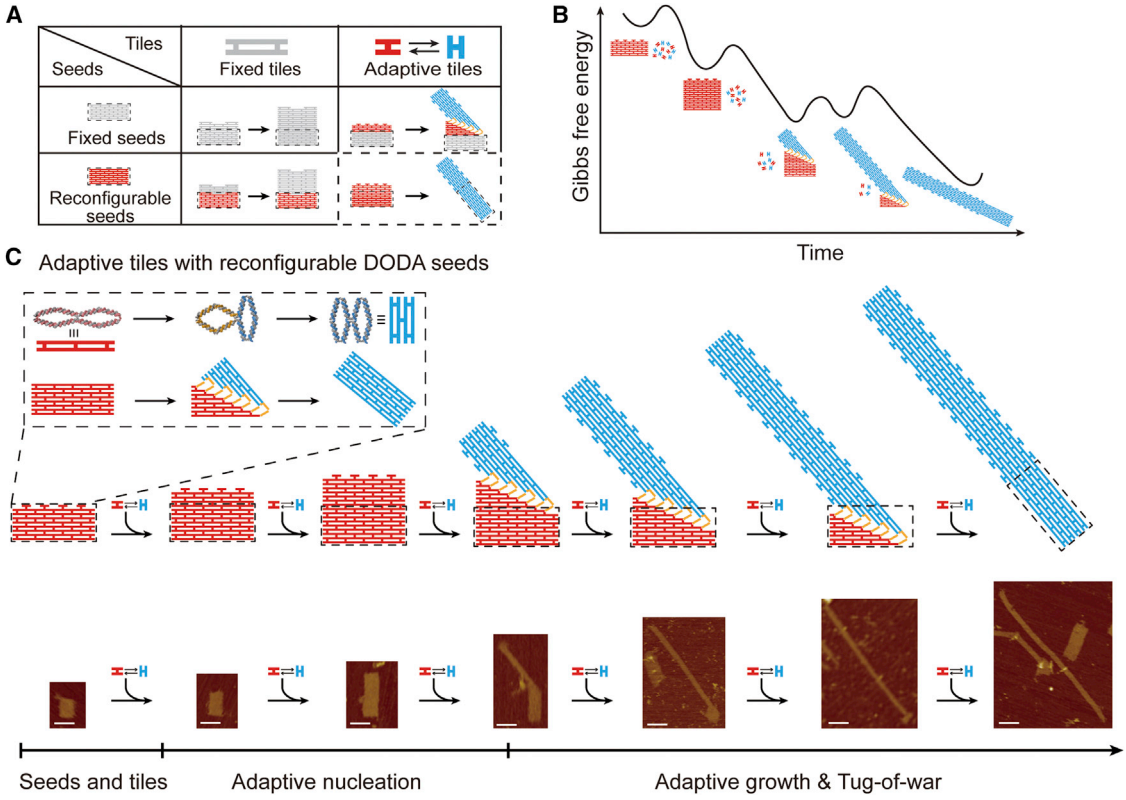

Figure 3. Seeded growth of adaptive DNA tiles on reconfigurable DNA origami seeds with tug-of-war behavior

(A) The difference in seeded growth between fixed and adaptive DNA tiles on fixed and reconfigurable seeds.

(B) Gibbs free energy versus the time during the adaptive DNA tiles assembling on reconfigurable DODA seeds.

(C) Process of adaptive nucleation and growth and the tug-of-war between adaptive tiles and reconfigurable DODA seeds. Note that the dashed box shows that the DODA seeds possessed the reconfigurable ability from red to blue conformation by external stimulus. Scale bars: 100 nm.

the adaptive DNA tiles effectively assembled on the DODA seeds mainly following the red conformation pathway, which was controlled by the DODA seeds (Figures S34 and S35). In addition, the length of the assembled structures was approximately 200 nm, and the longest length was up to 450 nm (Figure S36).

The previous studies[15,25,32] showed that the tile growth prefers to be in the direction of DNA double helix axes, due to the lower free energy associated with such growth. Similarly, the growth of adaptive DNA tiles may result in the change in relative energy difference between red and blue conformations during the growth, causing the growing tile lattice to transform to the conformation that contains fewer DNA helices (blue conformation). From the results in Figure 2, increasing the tiles concentration could regulate the growth process, so we next investigated whether the high concentration of tiles could induce structural transformations on the assembled structures.

By increasing the adaptive tiles amount (500 nM), not all of the assembled structures were locked in red conformation, and the intermediate conformation (the structures partially transformed to blue conformation) gradually arose (Figures S37–S39). Furthermore, the blue configuration structure occasionally appeared in low yield (Figures S37 and S38), which demonstrated the possibility of the controllably conformational transformation on DODA seeds. With sufficient adaptive DNA tiles (>700 nM), the assembled structures successfully transformed to blue conformation

Please cite this article in press as: Liu et al., Seeded growth of adaptive tiles on DNA origami, Cell Reports Physical Science (2022), https://doi.org/10.1016/j.xcrp.2022.101040

(Figures S40 and S41). From the dashed box in Figure 3C, the DODA seeds composed of the correlative dynamic units. At first, the initial dynamic units were in unlocked states. After the trigger by the transformed growing tile lattice, the units could convert from the initial state (red configuration) to a different state (blue configuration). Based on the cascade transduction of units, the whole structure of DODA could transform from the red configuration to the blue configuration by simultaneously changing the direction of the DNA helix. The average length of the blue configuration structures was >600 nm, and the longest was >1.5 μm (Figure S42). In addition, quantitative yields of the red and blue structures were analyzed. As shown in Figure S43, with more tiles assembling on the dynamic seeds, the yield of the blue conformation gradually improved, indicating the effective transformation of the red conformation structures. The Gibbs free energy versus the time during the growth process was analyzed to further show this process. As illustrated in Figures 3B and S44, the assembled structures, including the DODA seeds, transformed to blue conformation in the continuous growth process, and exhibited an underlying tug-of-war competition mechanism between the adaptive tiles and DODA seeds, when the two conformations were in competition. Originally, the red conformation was more favorable than the blue, and the conformation was stabilized in red. By increasing the strength in blue, the structural conformation could transform from red to blue, which can even lead to the conformational change of DODA seeds. The transformations under the growth process and their representative AFM images are shown in Figure 3C. Most of the continuous transformations started from a corner of the assembled structures and propagated through a diagonal pathway, revealing an efficient assembly of the adaptive DNA tiles on DODA seeds and a successful tug-of-war process between adaptive DNA tiles and reconfigurable DODA seeds.

Application in the fluorescence resonance energy transfer (FRET) system

We applied the FRET system to demonstrate the pathway of energy transfer by using the dynamic switch from red to blue nanostructures. As a conceptual illustration, we introduced the Cy3- and Cy5-modified DNAs to functionalize the adaptive tiles, and the Cy3 and Cy5 were put on the adjacent units. As shown in Figure S45, in the red conformation, the distance between the adjacent Cy3 and Cy5 is approximately 17.8 nm (52-bp length DNA), making low FRET efficiency. With more tiles, the assembled structures transformed to the blue conformation, and the distance between the adjacent Cy3 and Cy5 was approximately 5 nm, showing high FRET efficiency.

As first, we applied the FRET system to the seeded growth on the fixed origami seeds. According to the AFM results and the transformation of the structures in Figure 2, we introduced a series of tiles concentration to show the FRET variations (Figure 4A). To show the effective assembly of the Cy3 and Cy5 on the adaptive tiles, we used agarose gel analysis. As shown in the UV channel of Figure 4B, with more tiles' assembly on the seeds, the origami bands were gradually weakened (lanes 1–5, gray dashed box), and effectively assembled structures may block the gel holes (lanes 1–5, red dashed box). Compared with the Cy3 and Cy5 channels, there are strong Cy3/Cy5 signals in the gel holes (lanes 4 and 5), and the Cy3 and Cy5 functionalized tiles (lane 7) were also successfully imaged in the corresponding channels, both showing the effectively assembly of the Cy3 and Cy5 on the seeds. Furthermore, we applied the fluorescence spectrometer to analyze the FRET efficiency during the seeded growth process. As demonstrated in Figure 4C, with more tile assembling on the seeds, the FRET efficiency improved, indicating the successful transformation of the assembled structures. In addition, we applied the FRET system to the seeded growth of the dynamic origami seeds. Similar to the results in Figure 4, with more adaptive tiles' growth on the dynamic origami seeds, the FRET efficiency also improved (Figure S46).

Please cite this article in press as: Liu et al., Seeded growth of adaptive tiles on DNA origami, Cell Reports Physical Science (2022), https://doi.org/10.1016/j.xcrp.2022.101040

CellPress
OPEN ACCESS

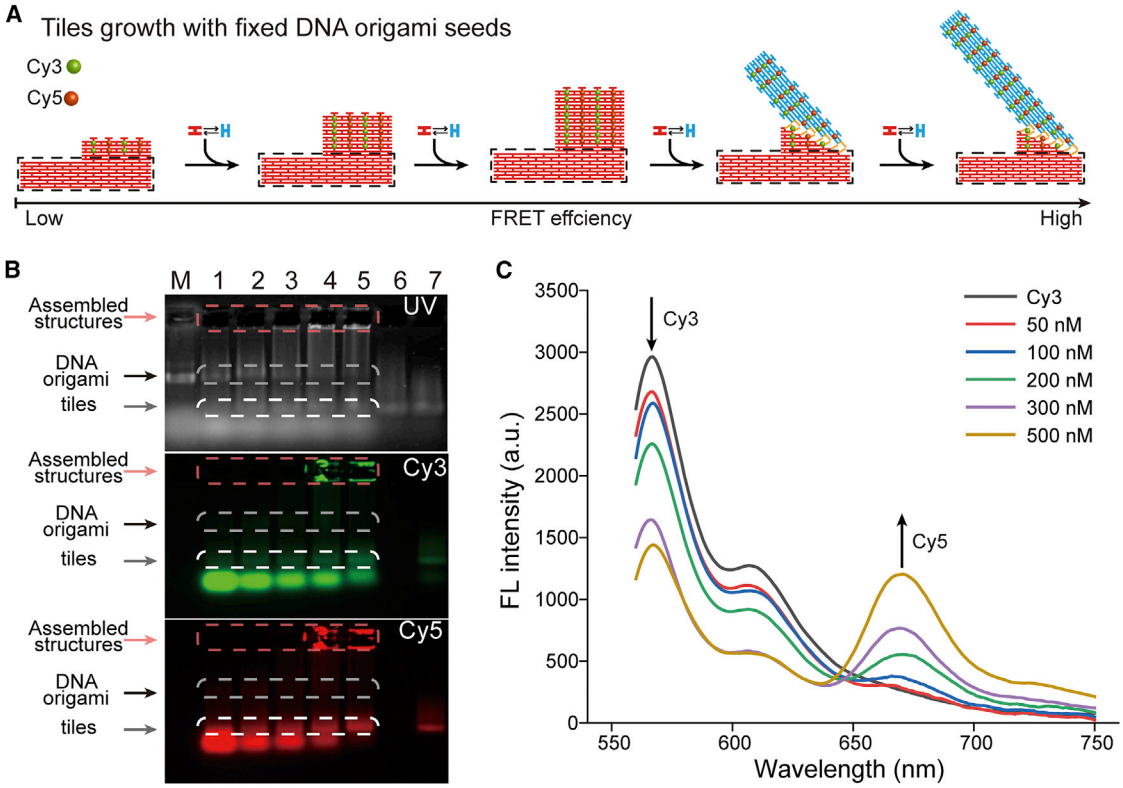

Figure 4. FRET analysis of the adaptive tiles' assembly on the fixed origami seeds

(A) The FRET efficiency improved with the structures transforming to the blue conformation (more tiles assembling on the fixed seeds).

(B) Agarose gel analysis of the adaptive tiles' assembly on the fixed origami seeds. M: fixed DNA origami seeds (10 nM); fixed DNA origami seeds with 50 nM (lane 1), 100 nM (lane 2), 200 nM (lane 3), 300 nM (lane 4), and 500 nM (lane 5) tiles; adaptive tiles without (lane 6) and with (lane 7) Cy3 and Cy5. The adaptive tiles were assembled by isothermal methods. Because the ethidium bromide can be excited at approximately 500 nm, the agarose gel was first imaged by Cy3 and Cy5 channels, and then negatively stained by 0.0001% (v/v) ethidium bromide buffer.

(C) Fluorescence (FL) spectra of the assembled structures under different tiles concentrations (50–500 nM).

DISCUSSION

In this work, we demonstrated a novel seeded growth strategy via the assembly of the adaptive DNA tiles on DNA origami seeds. The assembly of the adaptive DNA tiles on the origami seeds was dynamically controlled in a programmable way through the assistance of DNA 4-arm junction units, which could transform between two staple configurations. Initially, the adaptability of the tiles was explored by adaptive DNA tiles or fixed DNA tiles assembling on two origami seeds. Unlike the fixed DNA tiles only assembling on one kind of seeds, the adaptive DNA tiles successfully assembled on the two kinds of origami seeds, demonstrating the adaptive assembly ability of adaptive DNA tiles. Moreover, the adaptive DNA tiles realized adaptive assembly on fixed origami seeds, but did not trigger the regulation of fixed origami seeds. In contrast, the adaptive DNA tiles assembling on reconfigurable DODA seeds further realized the whole DODA seeds changing to blue conformation, and tug-of-war between the adaptive DNA tiles and DODA seeds after adequate tiles on the seeds.

Compared to the previous strategies that focused on the fixed DNA structures,[15,25,26,29,32] the dynamic DNA structures spotlighted in this study demonstrated a distinct reconfigurable performance.[39–42] The exploit of adaptive seeded growth manner and tug-of-war process benefits from the two dynamic properties

Please cite this article in press as: Liu et al., Seeded growth of adaptive tiles on DNA origami, Cell Reports Physical Science (2022), https://doi.org/10.1016/j.xcrp.2022.101040

of the reconfigurable DNA system. (1) The conformational transformation ability of the reconfigurable DODA seeds and adaptive DNA tiles. The controllable, multi-step, and cascade transformation allows the further long-range configurational change of the structure; (2) the preferred parallel nucleation orientation along with the helix orientation of the structures.[15,25,32] It further enabled the transformation of reconfigurable DNA structures without the help of DNA triggers. The utilization of reconfigurable DNA origami[43–46] in this research achieved coupling of active, controllable, and dynamic DNA devices with adaptive properties.

We believe that our adaptive seeded growth strategy could lend insights into responsive materials with sensing and reconfigurable properties,[47–49] owing to adaptive DNA tiles and reconfigurable DODA architectures.[50–52] The structural transformation could be realized by interconnected sensing and regulating components (4-arm junction units), which bring the controllable and flexible manipulation to the final materials. Moreover, such reconfigurable architectures could be further functionalized by designated components, such as nanoparticles[53,54] (e.g., AuNPs, AgNPs), proteins,[55,56] and other molecules[57,58] to acquire responsive capability. Meanwhile, the strategy proposed here provided fundamental support for the new mechanism of constructing and regulating the complex DNA nanomachines.[59–61]

EXPERIMENTAL PROCEDURES

Resource availability

Lead contact

Further information and requests for resources should be directed to the lead contact, Jie Song (sjie@sjtu.edu.cn).

Materials availability

This study did not generate new unique reagents.

Data and code availability

All data reported in this article are available in the supplemental information.

Materials

All of the other short DNA strands (staple DNA strands) were purchased from Sangon Biotech (Shanghai, China). All of the DNA strands used in this study were shown in Tables S1, S2–S10, S11, S12–S23, S24, S25, S26. Reagents for electrophoresis analysis by agarose gels were ethidium bromide (Sigma-Aldrich, cat. no. E1510), 10× loading buffer (Takara, cat. no. AH20611A).

Assembly of DNA origami seeds and DNA tiles

The design diagrams of the DNA origami seeds or DNA tiles were shown in Figures S47-S52. And the detailed assembly methods and the purification methods can be seen in the following or in the Supplemental Experimental Procedures.

For DNA origami: Staple DNA strands (100 nM each) and scaffold DNA strands with the concentration ratio 10:1 were mixed in TE/Mg^{2+} buffer (40 mM Tris base, 1 mM EDTA, and 12.5 mM magnesium acetate, pH 8.0). The mixtures were stepwise cooled down (at 95°C for 5 min, 85°C–25°C using a linear cooling ramp at the rate of 5 min/°C, and then 12°C forever). The samples were first confirmed by agarose, and then further identified by AFM.

Please cite this article in press as: Liu et al., Seeded growth of adaptive tiles on DNA origami, Cell Reports Physical Science (2022), https://doi.org/10.1016/j.xcrp.2022.101040

For DNA tiles: Blue DNA strands (200 nM each), gray DNA strands (200 nM each), and green DNA strands (200 nM each) with a concentration ratio of 1:1 were mixed in TE/Mg^{2+} buffer. The mixtures were stepwise cooled down (at 95°C for 5 min, 85°C–25°C using a linear cooling ramp at the rate of 2 min/°C, and then 12°C forever).

Isothermal assembly of the origami seeds with DNA tiles

First, the seeds and the DNA tiles were formed by the one-pot annealing method, then the sample was purified by filters, and qualified by NanoDrop. Second, the DNA tiles and the origami seeds were added together with the concentration ratios of 10:1, 20:1, 30:1, 50:1, and 70:1. Third, the connector DNA strands (gray and green) that connected the seeds and tiles and green strands (linking the repetitive tile monomer) were added to the mixture. Finally, the mixture was incubated at 60°C for 20 h, and then 12°C forever. After that, the samples were purified by filter at least 3–6 times.

SUPPLEMENTAL INFORMATION

Supplemental information can be found online at https://doi.org/10.1016/j.xcrp.2022.101040.

ACKNOWLEDGMENTS

The authors are grateful for the financial support from the National Natural Science Foundation of China (nos. 81822024 and 22161132008), the Natural Science Foundation of Shanghai, China (nos. 19520714100 and 19ZR1475800), the Project of Shanghai Jiao Tong University (nos. 2019QYA03 and YG2017ZD07), and the startup funding from Institute of Basic Medicine and Cancer (IBMC), Chinese Academy of Sciences (2020QD04). We also acknowledge the Shared Instrumentation Facility at the Institute of Basic Medicine and Cancer (IBMC), Chinese Academy of Sciences and Zhiyuan Innovative Research Center, SJTU.

AUTHOR CONTRIBUTIONS

Conceptualization, J.S. and Y.K.; methodology, Y.L.; investigation, Y.L.; writing – original draft, Y.L.; writing – review & editing, J.S., Y.K., Y.L., J.C., Y.W., and Y.X.; visualization, Y.L., J.S., Y.K., K.Z., L.T., Y.X., and D.C.; funding acquisition, J.S.; supervision, J.S. and Y.K.

DECLARATION OF INTERESTS

The authors declare no competing interests.

Received: May 21, 2022
Revised: August 5, 2022
Accepted: August 15, 2022
Published: September 1, 2022

REFERENCES

1. Seeman, N.C. (1982). Nucleic acid junctions and lattices. J. Theor. Biol. *99*, 237–247.
2. Nummelin, S., Kommeri, J., Kostiainen, M.A., and Linko, V. (2018). Evolution of structural DNA nanotechnology. Adv. Mater. *30*, e1703721.
3. Ke, Y., Castro, C., and Choi, J.H. (2018). Structural DNA nanotechnology: artificial nanostructures for biomedical research. Annu. Rev. Biomed. Eng. *20*, 375–401.
4. Rothemund, P.W.K. (2006). Folding DNA to create nanoscale shapes and patterns. Nature *440*, 297–302.
5. Yin, P., Hariadi, R.F., Sahu, S., Choi, H.M.T., Park, S.H., Labean, T.H., and Reif, J.H. (2008). Programming DNA tube circumferences. Science *321*, 824–826.
6. Wei, B., Dai, M., and Yin, P. (2012). Complex shapes self-assembled from single-stranded DNA tiles. Nature *485*, 623–626.
7. Ke, Y., Ong, L.L., Shih, W.M., and Yin, P. (2012). Three-dimensional structures self-assembled from DNA bricks. Science *338*, 1177–1183.
8. Zhang, Y., Pan, V., Li, X., Yang, X., Li, H., Wang, P., and Ke, Y. (2019). Dynamic DNA structures. Small *15*, e1900228.
9. Douglas, S.M., Chou, J.J., and Shih, W.M. (2007). DNA-nanotube-induced alignment of membrane proteins for NMR structure determination. Proc. Natl. Acad. Sci. USA *104*, 6644–6648.

Please cite this article in press as: Liu et al., Seeded growth of adaptive tiles on DNA origami, Cell Reports Physical Science (2022), https://doi.org/10.1016/j.xcrp.2022.101040

10. Tikhomirov, G., Petersen, P., and Qian, L. (2017). Fractal assembly of micrometre-scale DNA origami arrays with arbitrary patterns. Nature *552*, 67–71.

11. Ke, Y., Ong, L.L., Sun, W., Song, J., Dong, M., Shih, W.M., and Yin, P. (2014). DNA brick crystals with prescribed depths. Nat. Chem. *6*, 994–1002.

12. Lin, C., Liu, Y., Rinker, S., and Yan, H. (2006). DNA tile based self-assembly: building complex nanoarchitectures. ChemPhysChem *7*, 1641–1647.

13. Wagenbauer, K.F., Sigl, C., and Dietz, H. (2017). Gigadalton-scale shape-programmable DNA assemblies. Nature *552*, 78–83.

14. Yao, G., Zhang, F., Wang, F., Peng, T., Liu, H., Poppleton, E., Šulc, P., Jiang, S., Liu, L., Gong, C., et al. (2020). Meta-DNA structures. Nat. Chem. *12*, 1067–1075.

15. Schulman, R., Yurke, B., and Winfree, E. (2012). Robust self-replication of combinatorial information via crystal growth and scission. Proc. Natl. Acad. Sci. USA *109*, 6405–6410.

16. Liu, W., Zhong, H., Wang, R., and Seeman, N.C. (2011). Crystalline two-dimensional DNA-origami arrays. Angew. Chem. Int. Ed. Engl. *50*, 264–267.

17. Rajendran, A., Endo, M., Hidaka, K., and Sugiyama, H. (2013). Control of the two-dimensional crystallization of DNA origami with various loop arrangements. Chem. Commun. *49*, 686–688.

18. Zhang, T., Hartl, C., Frank, K., Heuer-Jungemann, A., Fischer, S., Nickels, P.C., Nickel, B., and Liedl, T. (2018). 3D DNA origami crystals. Adv. Mater. *30*, e1800273.

19. Li, W., Yang, Y., Jiang, S., Yan, H., and Liu, Y. (2014). Controlled nucleation and growth of DNA tile arrays within prescribed DNA origami frames and their dynamics. J. Am. Chem. Soc. *136*, 3724–3727.

20. Mohammed, A.M., and Schulman, R. (2013). Directing self-assembly of DNA nanotubes using programmable seeds. Nano Lett. *13*, 4006–4013.

21. Hamblin, G.D., Rahbani, J.F., and Sleiman, H.F. (2015). Sequential growth of long DNA strands with user-defined patterns for nanostructures and scaffolds. Nat. Commun. *6*, 7065.

22. Pfeifer, W., and Saccà, B. (2016). From nano to macro through hierarchical self-assembly: the DNA paradigm. Chembiochem *17*, 1063–1080.

23. Dunitz, J.D., and Bernstein, J. (2002). Disappearing polymorphs. Acc. Chem. Res. *28*, 193–200.

24. Holmes, J.D., Johnston, K.P., Doty, R.C., and Korgel, B.A. (2000). Control of thickness and orientation of solution-grown silicon nanowires. Science *287*, 1471–1473.

25. Barish, R.D., Schulman, R., Rothemund, P.W.K., and Winfree, E. (2009). An information-bearing seed for nucleating algorithmic self-assembly. Proc. Natl. Acad. Sci. USA *106*, 6054–6059.

26. Zhang, Y., Reinhardt, A., Wang, P., Song, J., and Ke, Y. (2020). Programming the nucleation of DNA brick self-assembly with a seeding strand. Angew. Chem. Int. Ed. Engl. *59*, 8594–8600.

27. Zhang, H., Wang, Y., Zhang, H., Liu, X., Lee, A., Huang, Q., Wang, F., Chao, J., Liu, H., Li, J., et al. (2019). Programming chain-growth copolymerization of DNA hairpin tiles for in-vitro hierarchical supramolecular organization. Nat. Commun. *10*, 1006.

28. Minev, D., Wintersinger, C.M., Ershova, A., and Shih, W.M. (2021). Robust nucleation control via crisscross polymerization of highly coordinated DNA slats. Nat. Commun. *12*, 1741.

29. Jiang, S., Pal, N., Hong, F., Fahmi, N.E., Hu, H., Vrbanac, M., Yan, H., Walter, N.G., and Liu, Y. (2021). Regulating DNA self-assembly dynamics with controlled nucleation. ACS Nano *15*, 5384–5396.

30. Schaffter, S.W., Scalise, D., Murphy, T.M., Patel, A., and Schulman, R. (2020). Feedback regulation of crystal growth by buffering monomer concentration. Nat. Commun. *11*, 6057.

31. Mao, X., Li, K., Liu, M., Wang, X., Zhao, T., An, B., Cui, M., Li, Y., Pu, J., Li, J., et al. (2019). Directing curli polymerization with DNA origami nucleators. Nat. Commun. *10*, 1395.

32. Woods, D., Doty, D., Myhrvold, C., Hui, J., Zhou, F., Yin, P., and Winfree, E. (2019). Diverse and robust molecular algorithms using reprogrammable DNA self-assembly. Nature *567*, 366–372.

33. Mohammed, A.M., Šulc, P., Zenk, J., and Schulman, R. (2017). Self-assembling DNA nanotubes to connect molecular landmarks. Nat. Nanotechnol. *12*, 312–316.

34. Song, J., Li, Z., Wang, P., Meyer, T., Mao, C., and Ke, Y. (2017). Reconfiguration of DNA molecular arrays driven by information relay. Science *357*, eaan3377.

35. Wang, D., Song, J., Wang, P., Pan, V., Zhang, Y., Cui, D., and Ke, Y. (2018). Design and operation of reconfigurable two-dimensional DNA molecular arrays. Nat. Protoc. *13*, 2312–2329.

36. Manuel García-Ruiz, J. (2003). Nucleation of protein crystals. J. Struct. Biol. *142*, 22–31.

37. Xu, J., Zhou, H., Yu, Q., Guerin, G., Manners, I., and Winnik, M.A. (2019). Synergistic self-seeding in one-dimension: a route to patchy and block comicelles with uniform and controllable length. Chem. Sci. *10*, 2280–2284.

38. Jun, Y.w., Choi, J.s., and Cheon, J. (2006). Shape control of semiconductor and metal oxide nanocrystals through nonhydrolytic colloidal routes. Angew. Chem. Int. Ed. Engl. *45*, 3414–3439.

39. Gerling, T., Wagenbauer, K.F., Neuner, A.M., and Dietz, H. (2015). Dynamic DNA devices and assemblies formed by shape-complementary, non-base pairing 3D components. Science *347*, 1446–1452.

40. Thubagere, A.J., Li, W., Johnson, R.F., Chen, Z., Doroudi, S., Lee, Y.L., Izatt, G., Wittman, S., Srinivas, N., Woods, D., et al. (2017). A cargo-sorting DNA robot. Science *357*, eaan6558.

41. Chatterjee, G., Dalchau, N., Muscat, R.A., Phillips, A., and Seelig, G. (2017). A spatially localized architecture for fast and modular DNA computing. Nat. Nanotechnol. *12*, 920–927.

42. Song, T., Eshra, A., Shah, S., Bui, H., Fu, D., Yang, M., Mokhtar, R., and Reif, J. (2019). Fast and compact DNA logic circuits based on single-stranded gates using strand-displacing polymerase. Nat. Nanotechnol. *14*, 1075–1081.

43. Fan, S., Wang, D., Cheng, J., Liu, Y., Luo, T., Cui, D., Ke, Y., and Song, J. (2020). Information coding in a reconfigurable DNA origami domino array. Angew. Chem. Int. Ed. Engl. *59*, 12991–12997.

44. Liu, Y., Cheng, J., Fan, S., Ge, H., Luo, T., Tang, L., Ji, B., Zhang, C., Cui, D., Ke, Y., and Song, J. (2020). Modular reconfigurable DNA origami: from two-dimensional to three-dimensional structures. Angew. Chem. Int. Ed. Engl. *59*, 23277–23282.

45. Wang, D., Yu, L., Ji, B., Chang, S., Song, J., and Ke, Y. (2020). Programming the curvatures in reconfigurable DNA domino origami by using asymmetric units. Nano Lett. *20*, 8236–8241.

46. Fan, S., Cheng, J., Liu, Y., Wang, D., Luo, T., Dai, B., Zhang, C., Cui, D., Ke, Y., and Song, J. (2020). Proximity-induced pattern operations in reconfigurable DNA origami domino array. J. Am. Chem. Soc. *142*, 14566–14573.

47. Liu, X., Yuk, H., Lin, S., Parada, G.A., Tang, T.C., Tham, E., de la Fuente-Nunez, C., Lu, T.K., and Zhao, X. (2018). 3D printing of living responsive materials and devices. Adv. Mater. *30*, 1870021.

48. Mellerup, S.K., and Wang, S. (2019). Boron-based stimuli responsive materials. Chem. Soc. Rev. *48*, 3537–3549.

49. Dai, Z., Leung, H.M., and Lo, P.K. (2017). Stimuli-responsive self-assembled DNA nanomaterials for biomedical applications. Small *13*, 1602881.

50. Daljit Singh, J.K., Luu, M.T., Abbas, A., and Wickham, S.F.J. (2018). Switchable DNA-origami nanostructures that respond to their environment and their applications. Biophys. Rev. *10*, 1283–1293.

51. Douglas, S.M., Bachelet, I., and Church, G.M. (2012). A logic-gated nanorobot for targeted transport of molecular payloads. Science *335*, 831–834.

52. Li, J., Johnson-Buck, A., Yang, Y.R., Shih, W.M., Yan, H., and Walter, N.G. (2018). Exploring the speed limit of toehold exchange with a cartwheeling DNA acrobat. Nat. Nanotechnol. *13*, 723–729.

53. He, L., Mu, J., Gang, O., and Chen, X. (2021). Rationally programming nanomaterials with DNA for biomedical applications. Adv. Sci. *8*, 2003775.

54. Liu, N., and Liedl, T. (2018). DNA-assembled advanced plasmonic architectures. Chem. Rev. *118*, 3032–3053.

Please cite this article in press as: Liu et al., Seeded growth of adaptive tiles on DNA origami, Cell Reports Physical Science (2022), https://doi.org/10.1016/j.xcrp.2022.101040

CellPress
OPEN ACCESS

55. Kong, G., Xiong, M., Liu, L., Hu, L., Meng, H.M., Ke, G., Zhang, X.B., and Tan, W. (2021). DNA origami-based protein networks: from basic construction to emerging applications. Chem. Soc. Rev. *50*, 1846–1873.

56. Dong, Y., Yao, C., Zhu, Y., Yang, L., Luo, D., and Yang, D. (2020). DNA functional materials assembled from branched DNA: design, synthesis, and applications. Chem. Rev. *120*, 9420–9481.

57. Fan, S., Wang, D., Kenaan, A., Cheng, J., Cui, D., and Song, J. (2019). Create nanoscale patterns with DNA origami. Small *15*, e1805554.

58. Ge, H., Wang, D., Pan, Y., Guo, Y., Li, H., Zhang, F., Zhu, X., Li, Y., Zhang, C., and Huang, L. (2020). Sequence-dependent DNA functionalization of upconversion nanoparticles and their programmable assemblies. Angew. Chem. Int. Ed. Engl. *59*, 8133–8137.

59. Heinen, L., and Walther, A. (2019). Programmable dynamic steady states in ATP-driven nonequilibrium DNA systems. Sci. Adv. *5*, eaaw0590.

60. Green, L.N., Subramanian, H.K.K., Mardanlou, V., Kim, J., Hariadi, R.F., and Franco, E. (2019). Autonomous dynamic control of DNA nanostructure self-assembly. Nat. Chem. *11*, 510–520.

61. Green, L.N., Amodio, A., Subramanian, H.K.K., Ricci, F., and Franco, E. (2017). pH-Driven reversible self-assembly of micron-scale DNA scaffolds. Nano Lett. *17*, 7283–7288.